JOURNAL OF PHYSICAL ORGANIC CHEMISTRY, VOL. 5, 518–528 (1992)

SELF-ORGANIZING SYSTEMS BASED ON AMPHIPHILIC CYCLODEXTRIN DIESTERS

PING ZHANG

CNRS SDI 6233, Laboratoire de Chimie Organique, Centre Pharmaceutique, Université de Paris Sud, 92290 Châtenay-Malabry, France

HÉLÈNE PARROT-LOPEZ

Laboratoire de Chimie Organique, Faculté de Pharmacie, Université de Paris V, 4 rue de l'Observatoire, 76006 Paris, France

PIERRE TCHORELOFF AND ADAM BASZKIN

CNRS URA 1218, Laboratoire de Physico-chimie des Surfaces, Centre Pharmaceutique, Université de Paris Sud, 92290 Châtenay-Malabry, France

CHANG-CHUN LING AND COLETTE DE RANGO

CNRS UPR 180, Laboratoire de Physique, Centre Pharmaceutique, Université de Paris Sud, 92290 Châtenay-Malabry, France

AND

ANTHONY W. COLEMAN*

CNRS SDI 6233, Laboratoire de Chimie Organique, Centre Pharmaceutique, Université de Paris Sud, 92290 Châtenay-Malabry, France

The formation of micelles, vesicles and monomolecular layers by amphiphilic cyclodextrins possessing hydrophobic ester groups on the secondary hydroxyl face is described. The physico-chemical properties of these self-organizing systems were studied by dynamic light scattering, variable-temperature ^{1}H NMR, the use of lanthanide shift reagents, deposition of Langmuir layers, variable-temperature solubility measurements and aqueous and non-aqueous surface tension activity measurements. The results are interpreted in terms of the cylindrical geometry of the compounds which, coupled with the presence of a large planar polar head group, leads to the formation of self-organized systems both in polar organic solvents and also at the air–water interface.

INTRODUCTION

The cyclodextrins are cyclic oligosaccharides possessing six, seven or eight α-1,4-linked glucopyranose units and forming a cylindrical molecule. The resultant non-polar cavity is capable of including a wide variety of organic molecules.[1] They are commercially available on the ton scale and have been widely used in alimentary,[2] pharmaceutical[3] and separation applications.[4]

Figure 1 shows the dimensions of α-, β- and γ-cyclodextrins and the molecular symmetries. In addition to the axial symmetry (C_n), the presence of two hydrophilic faces (the primary and secondary hydroxyl groups) surrounding a hydrophobic cavity, yields a 'face to face' pseudo-symmetry. In order to synthesize amphiphilic cyclodextrins, one of these two hydroxyl faces must be selectively substituted by hydrophobic groups (Figure 2). The synthetic strategies necessary to achieve this have been developed in the context of an interdisciplinary approach to new cyclodextrin derivatives, and a wide range of amphiphilic cyclodextrins are now available at the multi-gram level.[5]

In this paper we report the physico-chemical properties of a series of amphiphilic cyclodextrins in which the secondary hydroxyl face has been rendered hydrophobic by the addition of lipophilic ester groups at the O-2 and O-3 positions.[6] These molecules possess, as a core, a rigid cylindrical geometry and are capable of forming a wide range of self-organizing structures: micelles, vesicles and mono- and multi-molecular layers; as would be expected, the behaviour of these

* Author for correspondence.

0894–3230/92/080518–11$10.50

Received 12 February 1992
Revised 13 April 1992

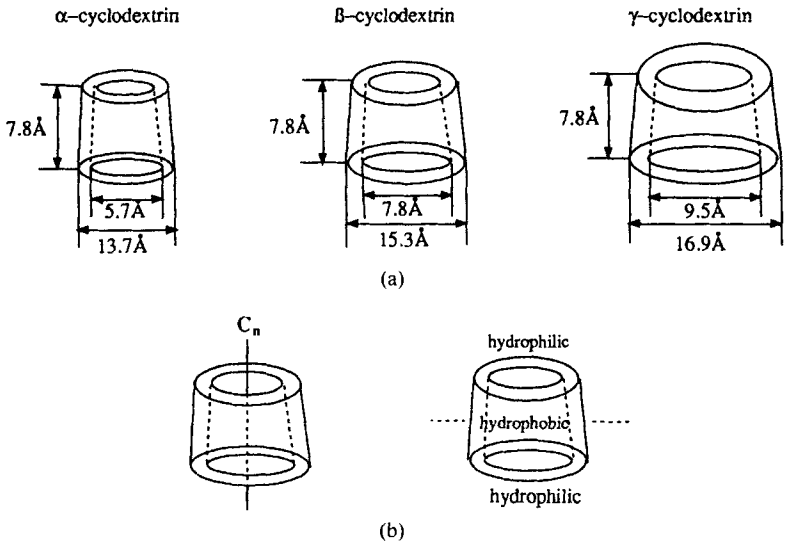

Figure 1. (a) Molecular dimensions and (b) molecular symmetries of cyclodextrins

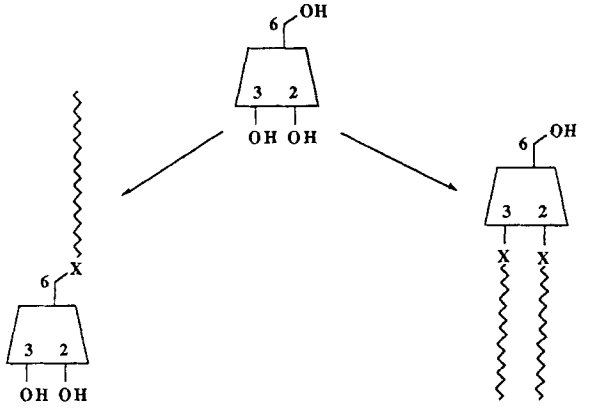

Figure 2. Synthetic strategy for the preparation of amphiphilic cyclodextrins

systems is dominated by the formation of lamellar structures.[7]

EXPERIMENTAL

The syntheses of amphiphilic CD diesters have been published previously for β-CD;[6,8] the α- and γ-CD derivatives were prepared by analogous methods[6] [α-CD-C14 ester, yield 66%, TLC $R_F = 0{\cdot}48$ (CH_2Cl_2–EtOH, 95 : 5); β-CD-C14 ester, yield 57%, $R_F = 0{\cdot}45$ (CH_2Cl_2–EtOH, 95 : 5); γ-CD-C14 ester, yield 51%, $R_F = 0{\cdot}42$ (CH_2Cl_2–EtOH, 95 : 5)].

Solvents were distilled over the appropriate drying agents prior to use and water was triply distilled. All glassware was cleaned with sulphuric acid–chromic acid mixture, abundantly rinsed with triply distilled water and dried before use.

Solubility measurements were carried out by placing a weighed amount of the compound in 5 ml of solvent in a stoppered tube, in a thermostated bath, and stirring at the desired temperature for 20 min. If complete dissolution occurred, a further amount was added and the experiment repeated until complete dissolution was no longer observed.

Surface tension was measured on a Prolabo T. D. 2000 tensiometer using the stirrup and blade technique. All measurements were repeated three times to ensure reproducibility. In the case of aqueous systems small (2 μl) volumes of a chloroform solution were deposited at the water surface and the solvent was allowed to to evaporate prior to the measurement. For measurements in tetrahydrofuran known amounts of the amphiphile were added to distilled tetrahydrofuran (THF).

^{1}H NMR measurements were carried out at 200 MHz on a Bruker AC 200 spectrometer. The signal was locked on the internal deuterium signals of the solvent and peaks were referenced with respect to the internal standard. Variable-temperature spectra were carried out at 5 K intervals between 293 and 363 K in pyridine-d_5 and between 293 and 343 K in THF-d_8.

External shift reagent experiments were carried by the addition of small amounts of $Eu(fod)_3$ or $Eu(NO_3)_3$ stepwise to solutions of the β-CD-C6 ester in THF-d_8 or pyridine-d_5.

Light-scattering experiments were carried out at various concentrations of the compound in THF or pyridine using a Coulter N4M Nanosizer. The measure-

ments were repeated three times to ensure reproducibility.

Monolayers of cyclodextrins were deposited at the air–water interface of a Langmuir-type film balance (MCN Lauda, Germany). Known concentrations of approximately 10^{14} molecules were deposited from chloroform solutions and were allowed to evaporate for 10 min before the compression π–A isotherms were recorded at a constant compression rate of $2{\cdot}3$ cm min^{-1}. The π–A isotherms were recorded at least three times to ensure that the molecular surface areas measured were within experimental error.

Molecular graphics studies were carried out using the SYBYL modelling package. The initial structures were constructed using cyclodextrin coordinates obtained from the Cambridge Crystallographic Data Bank. The chains were added in a geometry which will correspond to a compact state, and an initial energy optimization was carried out using the internal force field. In a second series of calculations, the O-2 chains were oriented towards the molecular cavity with the O-3 chains remaining oriented towards the exterior, giving an 'in–out' conformation. For the non-compact state no energy minimization was carried out and the figure is only a simplified representation.

RESULTS

Temperature dependence of solubility

Figure 3 shows the solubilities of the β-CD-C6, β-CD-C12 and β-CD-C14 O2, O3-diesters in THF as a function of temperature. The designation C6, C12 and C14 refers to the ester chain length.

Solubilities at 20 °C for the compounds are β-CD-C6 = 450 β-CD-C12 = 360 and β-CD-C14 = 310 g l^{-1}; the solubilities increase slowly up to 50 °C, at which temperature all three compounds have essentially the same solubility of 500 g l^{-1}. A sharp increase in solubility occurs above this value, reaching 850 g l^{-1} for β-CD-C6, 940 g l^{-1} for β-CD-C12 and 1410 g l^{-1} for β-CD-C14 at 60 °C. It is noteworthy that the break point for all three compounds occurs at identical temperatures. This suggests that the process occurring is related to a single constant factor, unrelated to the alkyl chain length (probably OH-6 head group interactions). As shown above, in the lower temperature zone the solubility is inversely related to chain length, C6 ≫ C12 > C14.

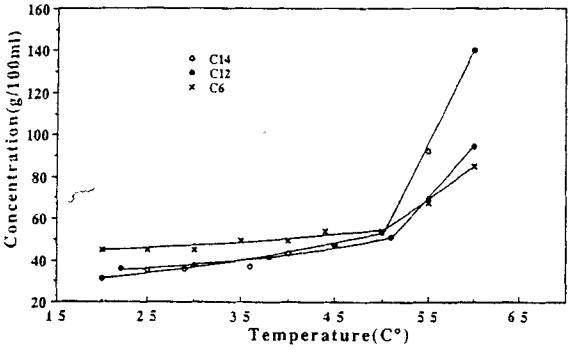

Figure 3. Solubility of the amphiphilic diesters β-CD-C6, β-CD-C12 and β-CD-C14 in tetrahydrofuran as a function of temperature

Surface tensions of aqueous solutions

Surface tension–concentration plots are given in Figure 4 for β-CD-C2 diester. This compound exhibits a strong surface activity, characterized by the appearance of the critical micellar concentration (CMC) value of concentration equal to 2×10^{-7} M. For *n*-octyl-β-glucoside[9] and sucrose monolaurate[10] the CMC values were found at concentrations much higher than that observed for β-CD-C2, $2{\cdot}5 \times 10^{-2}$ and $3{\cdot}4 \times 10^{-4}$ M, respectively.

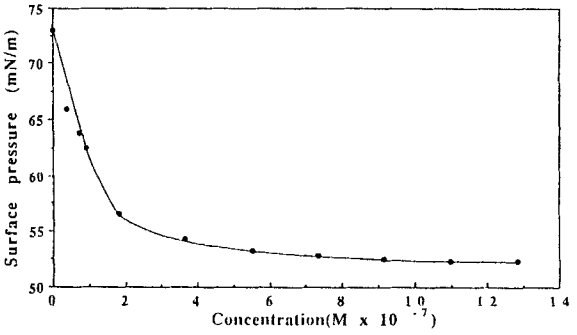

Figure 4. Concentration dependence of the surface tension of β-CD-C2 in water

Surface tensions of tetrahydrofuran solutions

Figure 5 shows the surface tension–concentration curves for β-CD-C6, β-CD-C12 and β-CD-C14 in THF.

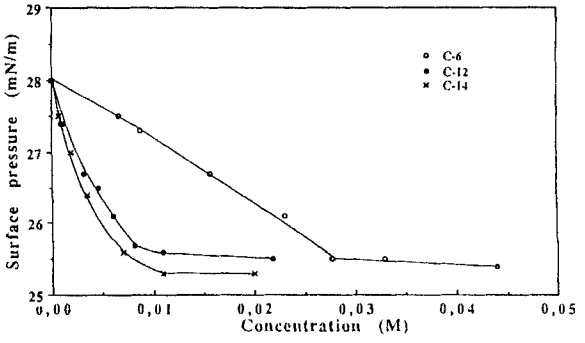

Figure 5. Concentration dependence of the surface tension of β-CD-C6, β-CD-C12 and β-CD-C14 in tetrahydrofuran

Although the effects are relatively small, they are reproducible. The curves obtained resemble closely those observed for surfactants in aqueous solutions (see Figure 4) and are all consistent with the formation of vesicles (cf. phospholipids). The critical micellar concentrations are $2{\cdot}8 \times 10^{-2}$ M for β-CD-C6, $7{\cdot}1 \times 10^{-3}$ M for β-CD-C12 and $6{\cdot}0 \times 10^{-3}$ M for β-CD-C14.

Dynamic light scattering

In view of the above results, which support the formation of micelles or vesicles in aqueous and non-aqueous systems, aggregate size was investigated by light scattering. For β-CD-C14 in pure THF, with a mean apparent diameter of 530 nm at a scattering angle of 90°, the aggregates are stable over a period of 48 h with no observed variation in size. In water–THF mixtures, at aqueous mole fractions of 1% and 2%, slightly smaller aggregates are observed at 420 nm diameter. For mole fractions in excess of 3% extremely large aggregates are observed, with apparent diameters in excess of 2100 nm. Diameters of around 400–500 nm are in accord with the curvature needed for the formation of vesicles, with a lamellar external membrane. Formation of vesicles in non-aqueous media is rare and only recently have liposomes been observed by electron microscopy from such solvents.[11]

For the β-CD-C12 and β-CD-C14 diesters in pyridine, much larger, highly disperse aggregates are observed of apparent diameter apparent *ca* 4300 nm. In contrast to the behaviour in THF, such systems in pyridine are relatively unstable and during 2 h further aggregation occurs, leading to assemblies larger than 10 μm.

Variable-temperature ^{1}H NMR studies

Variable-temperature ^{1}H NMR studies have been widely used to provide information about solvent accessibility of proton[12] and phase changes in organized systems. Here we used this technique to provide information on the structure of the bilayers formed by aggregates of the CD diesters.[13]

Tetrahydrofuran

The room-temperature ^{1}H NMR spectra of the β-CD-C6, β-CD-C12 and β-CD-C14 diesters in THF-d_8 are broadened with no differentiation observed between the O-2 and O-3 chain CH_2 or CH_3 protons. In this solvent, the OH-6 [Figure 6(a)] and H_2O slope [Figure 7(a)] signals are relatively insensitive to temperature.

The temperature/chemical shift slope for OH-6 of *ca* 1·4 Hz °C^{-1} suggesting a system in which there is little interaction between the OH-6 head group and the solvent. This situation is similar to that observed for peptides and proteins in which amide resonances are temperature invariant for buried amide groups.[12] This is in accord with the observed residual water possibly bridging hydroxyl groups as observed in the solid state for the native cyclodextrins.[14]

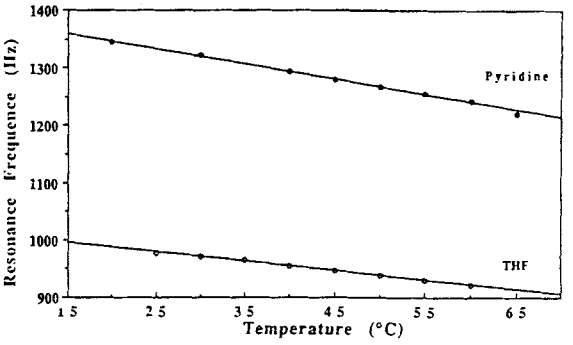

Figure 6. Tempreature dependance of the OH-6 ^{1}H NMR resonance in (a) tetrahydrofuran-d_8 and (b) pyridine-d_5 for β-CD-C6

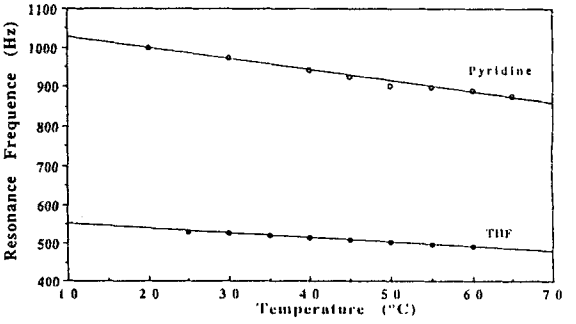

Figure 7. Temperature dependance of H_2O ^{1}H NMR resonance in (a) tetrahydrofuran-d_8 and (b) pyridine-d_5 for β-CD-C6

Pyridine

In pyridine-d_5, for the β-CD-C6 diester, the OH-6 signal is relative easily identified as occurring 6·7 ppm at 20 °C. At room temperature the CH_2 chain protons are observed as relatively broad peaks, centred at 1·34 and 1·50 ppm. The CH_3 protons are observed as two triplets at 0·89 and 1·01 ppm, hence we now observe inequivalence between the O-2 and O-3 chains.

Both the OH-6 [Figure 6(a)] and water [Figure 7(b)] resonances are more temperature sensitive than in THF-d_8, showing slopes of 2·7 and 2·8 Hz °C^{-1}, respectively. This probably arises from solvent–head group interactions. Separate resonances are observed in the O-2 and O-3 chains for the CH_2 chain and CH_3

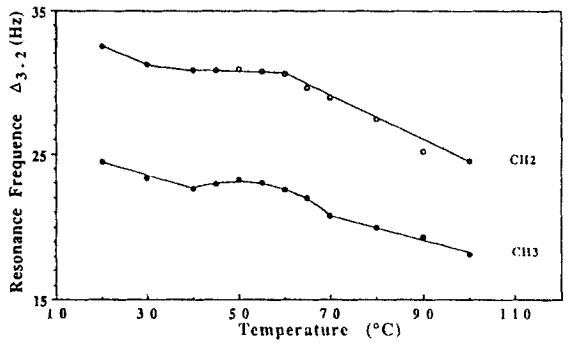

Figure 8. Temperature dependence of the frequency difference of O-2 and O-3 CH_3 and CH_2 chain resonances in the ^1H NMR spectra of β-CD-C6

protons [Figure 8(b)]; this would be the case for molecules packed in a classical bilayer assembly in which the alkyl chains will be sterically non-equivalent; in this aggregate structure, the polar head groups will be oriented towards the solvents. Figure 8 presents the chemical shift differences between the O-2 and O-3 CH_2 chain and CH_3 terminal peaks.

The curves for the chemical shift difference between the O-2 and O-3, CH_2 chain and CH_3 terminal protons show zones of 30–60 °C (CH_2 chain) and 40–70 °C (CH_3 terminal) in which there is considerable divergence from a linear variation. The slopes observed in the regions outside these areas are $\Delta = 0{\cdot}13$ Hz °C^{-1} for CH_2 and $\Delta = -8 \times 10^{-2}$ Hz °C^{-1} for CH_3. Such changes in chemical shift differences may arise from a change in the phase state of the chains, possibly a passage from a static to a dynamic state for one or both ester chain groups.

External shift reagents

The addition of $Eu(fod)_3$ or $Eu(NO_3)_3$ to β-CD-C6 in pyridine-d_5 caused the OH-6 resonance to be displaced (0·6 ppm) and broadened; eventually at high concentrations the resonance is so broadened as to be unobserved. No other perturbations of the ^1H NMR spectrum were observed.

In THF-d_8 the addition of $Eu(fod)_3$ causes perturbation of the CH_2 and CH_3 resonances, with some splitting of the peaks occurring. For $Eu(NO_3)_3$ at low concentrations of the shift reagent the CH_2 and CH_3 resonances are again perturbed, but at higher concentrations the OH-6 resonance is now broadened and shifted (0·4 ppm).

Surface pressure–area isotherms of monomolecular layers

Figure 9 gives the surface pressure π(mN m^{-1}) versus molecular area (Å^2) curves for deposited layers of α-CD-C14, β-CD-C14 and γ-CD-C14 diesters. The curves show two distinct parts in which a rise in π is observed. The first corresponds to the expanded state of the film, A_0, and arises from the compact state. Extrapolation of these linear parts to the abscissa yields molecular area A_0 values (I) of 334 398 and 441 Å^2 and A values (II), of 288, 338 and 385 Å^2 (Table 1). Dividing the corresponding A_0 or A values by the number of chains for each compound gives a mean area per chain equal to 28 (±0·1) Å, characteristic of compounds in the non-compact state (I) and 24·0 (±0·1) Å in their compact form (II). All three compounds form stable layers with collapse pressures for α-CD-C14 and β-CD-C14 of 44·6 and 43·1 mN m^{-1}, respectively, and γ-CD-C14 of 47 mN m^{-1}. The shape of the π–A isotherms suggests that transitions from liquid expanded to liquid condensed and solid states of monolayers take place.[15]

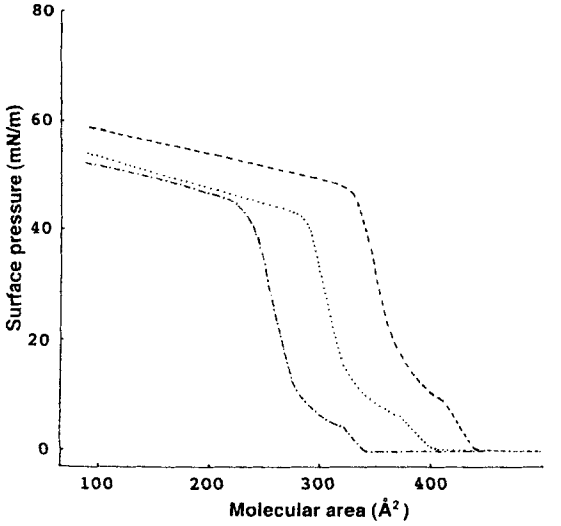

Figure 9. Surface pressure isotherms for the diesters _____ α-CD-C14, ... β-CD-C14 and _._._._ γ-CD-C14 at the air–water interface

The surface pressure isotherms for β-CD-C2, β-CD-C6, β-CD-C8, β-CD-C10 and β-CD-C12 are shown in Figure 10. The compounds show A_0 values as follows: C2, $A_0 = 314$ Å^2 mean chain area 22·4 Å^2; C6 $A_0 = 337$ Å^2, mean chain area 24·1 Å^2; C8, $A_0 = 356$ Å^2; C10, $A_0 = 361$ Å^2; and C12, $A_0 = 368$ Å^2. The corresponding mean area per chain is 25·4, 25·8 and 26·3 Å^2, respectively. The collapse pressure values for C6, C8, C10 and C12 are approximately the same at 30·5 mN m^{-1}, whilst the monolayer formed by β-CD-C2 is less stable with a collapse pressure of only 14 mN m^{-1}.

The observed values of A (compact) for α-CD-C14 (288 Å^2), β-CD-C14 (338 Å^2) and γ-CD-C14 (385 Å^2) are consistently larger than those observed for amaphiphilic cyclodextrins in which lipophilic group is

Table 1. Result from compression isotherms of amphiphilic molecules

Compound	Molecular area, A(Å^2) Experimental	Calculated	Collapse pressure (mN m^{-1})	Area per alkyl chain area, A (Å^2)	Collapse pressure per alkyl chain area (Å^2)
α-CD-C14	288, 334[a]	339	44·6	24·0, 28·0[a]	19·1
β-CD-C14	338, 398[a]	407	43·1	24·1, 28·4[a]	20·2
γ-CD-C14	385, 441[a]	450	47·0	24·1, 28·0[a]	20·3
β-CD-C12	368	379	30·1	26·3	20·6
β-CD-C10	361	358	30·1	25·8	20·0
β-CD-C8	356	351	30·6	25·4	18·4
β-CD-C6	337	323	33·0	24·1	18·0
β-CD-C2	314	289	14·0	22·4	16·0[b]

[a] Expanded (fluid state)(A_0).
[b] The line shape for β-CD-C2 reeduces the accuracy for these values.

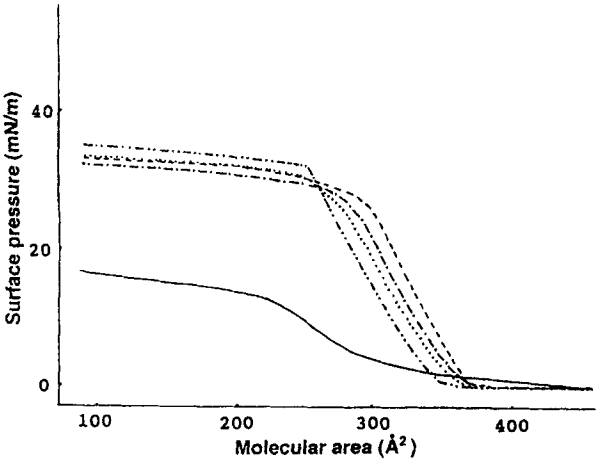

Figure 10. Surface pressure isotherms for the diesters __ β-CD-C2, __.__.__.__ β-CD-C6, ... β-CD-C8, __.__.__ β-CD-C10 and _____ β-CD-C12 at the air–water interface

attached at the primary face;[5,16] for the aminoalkyl-CDs, α-CD-NH-C16 = 162 Å^2, β-CD-NH-C16 = 215 Å^2 and γ-CD-NH-C16 = 287 Å^2.

From the observed values it is possible to calculate the areas occupied per chain for each conformation for the C14 diesters. The extended and compact areas obtained are constant for α-, β- and γ-CD at 28·0 and 24·1 Å^2, respectively. The values obtained at the collapse pressures are 19·1, 20·2 and 20·3 Å^2, respectively, and are close to the hydrocarbon cross-sectional area of 20 Å^2. The values obtained are slightly smaller than those observed by Taneva *et al.*[16] for the aminoalkyl-CDs, but consistent with the structure of these compound containing a slightly wider cavity at the secondary face which allows a compact final packing arrangement. The molecular areas observed at the collapse pressure increase with increasing chain length.

Molecular graphics

In Table 2 are given the calculated molecular diameters for 'compact' forms of the diesters, along with the

Table 2. Molecular graphics results

Compound	Chain length (Å)	CD diameter (Å)	Calculated energy (kcal mol^{-1})	Van der Waals energy (kcal mol^{-1})
α-CD-C14	16·702	20·780	−79·408	−155·929
β-CD-C14	16·702	22·765	−96·222	−180·830
γ-CD-C14	16·702	23·941	−74·923	−216·802
β-CD-C12	14·215	21·972	−86·568	−163·071
β-CD-C10	11·351	21·356	−90·048	−159·483
β-CD-C8	8·850	21·147	−56·753	−137·820
β-CD-C6	6·491	20·286	−38·182	−115·060
β-CD-C2	1·510	19·074	−2·017	−61·049
β-CD-C2(in)	1·510	15·738	82·745	−42·561
β-CD-C14[a]	16·702	18·862	−118·423	−219·600

[a] This structure corresponds to a highly compact state, probably observed near the collapse pressure.

minimum energy values, values for the van der Waals energies and the chain length and the corresponding values for the 'in–out' mode for β-CD-C14. In Figure 11 are shown space filling representations of α-CD-C14, β-CD-C14 and γ-CD-C14, parallel and perpendicular to the molecular C_n axis for the non-compact form.

The calculated values for A_0 and A, as shown in Table 2, are in close agreement with the observed values. The observed increase in molecular diameter

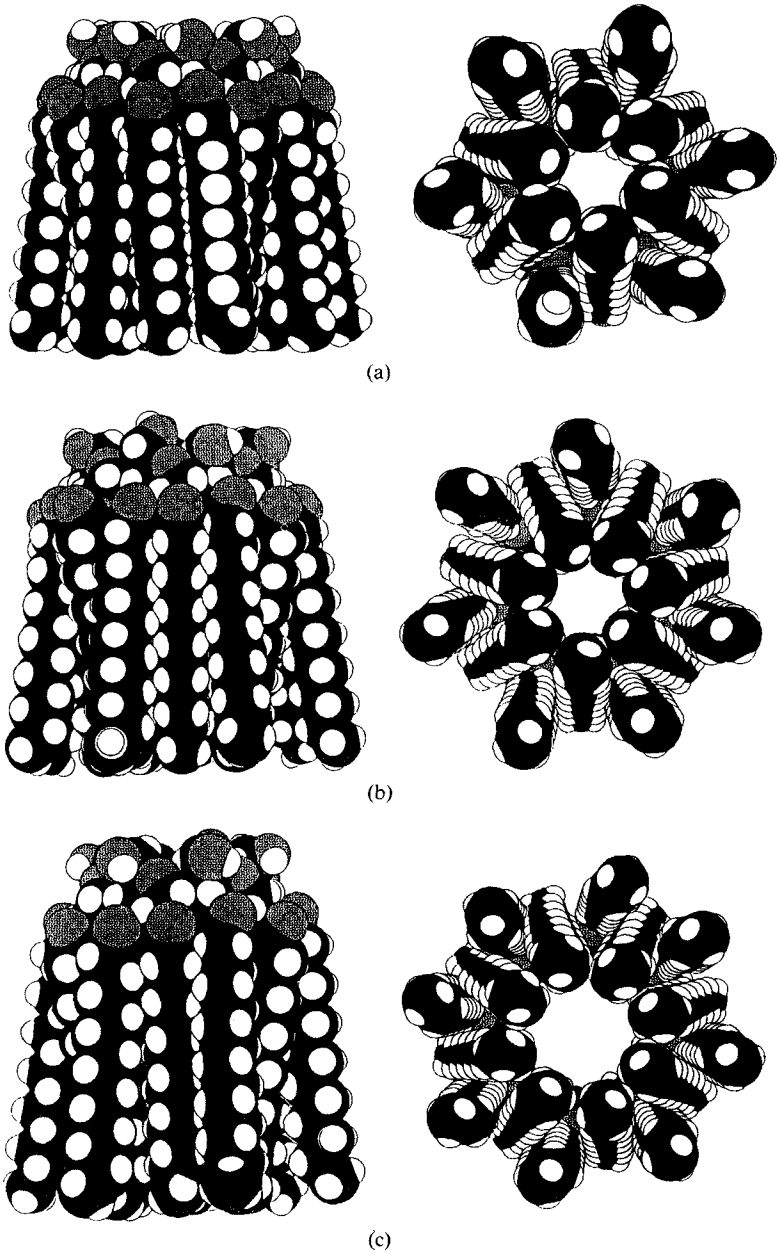

Figure 11. Molecular graphics representations of the diesters (a) α-CD-C14, (b) β-CD-C14 and (c) γ-CD-C14 in the non-compact mode

with increasing chain length results from a geometry in which the O-3 chains are oriented slightly outwards from the molecular axis. This geometry leaves an open cavity with a relatively open-chain packing, corresponding to a mean chain area which should be larger than that of close-packed alkyl chains, i.e. > 20 Å^2, in agreement with the observed value of 24 Å^2 for A. The overall geometry is that of a cylindrical hydrophobic zone capped by a conical polar zone (CD + ester carbonyl) *ca* 6·5 Å in depth. The ester carbonyl oxygen atoms are clearly available for interaction with the external environment.

The 'in–out' conformations in which the O-2 ester linkage moves to the interior of the cavity may be expected to correspond to those observed in the compression zone in which the chains will rearrange geometry until increasing van der Waals repulsion will prevent further molecular compaction. In this geometry the chains are packed in a dense form where the mean chain area will approach the value of 20 Å^2 typical for single close-packed alkyl forms.

For β-CD-C2 a model was constructed with all acetate groups oriented in the 'in' mode. Energy calculations show very large repulsive energies for this conformation (*ca* 90 kcal mol^{-1}). Hence we may consider the 'in–out' mode as representing the most compact form possible.

DISCUSSION

The cyclodextrin O-2, O-3 diesters possess rigid cylindrical structures and hence self-organizing assemblies based on these molecules should be based on lamellar bilayer structures. From the dynamic light-scattering studies the molecules form large, uni- or multi-lamellar, vesicle structures in THF (500 nm).

In THF the evidence from the temperature dependence of solubility and the ^{1}H NMR chemical shift of the OH-6 protons leads us to propose an aggregate structure in which there are strong inter- and intramolecular interactions; when there are strong head group–head group interactions, the interactions will be via hydrogen bonding either directly between two hydroxyl groups or via the residual water molecules. It is expected that such hydrogen bonding will be intra- and intermolecular, with the intermolecular hydrogen bonding within the same layer and also spanning head groups or adjacent layers. Thus the change occurring at 50 °C implies a change in such interactions; this is in agreement with work of Jeffrey and Maluszynska[17] on certain mono-saccharide liquid crystal systems in which it was found that head group–head group rearrangements occur in self-assemblies of carbohydrate amphiphiles. This implies that in multimolecular assemblies there is a geometry with the polar head groups interacting and the hydrophobic chains oriented towards the solvent, i.e. a reversed membrane structure (Figure 12).

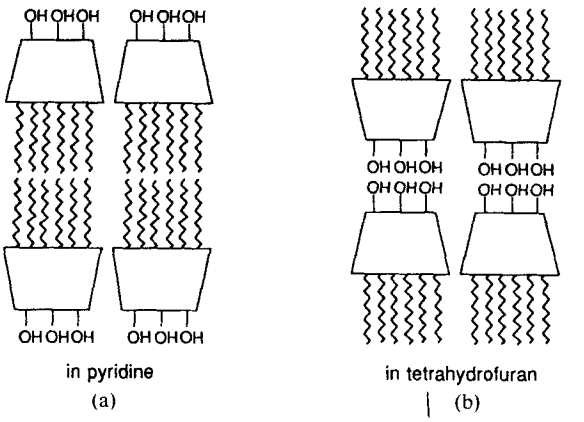

Figure 12. Proposed lamellar structure of the amphiphilic diesters in (a) tetrahydrofuran and (b) pyridine

In pyridine much larger objects (4000 nm) are formed; the exact nature of these is undetermined. However, the premise of a normal bilayer with the polar head group oriented towards the solvent is in accord with the observed effects in variable-temperature ^{1}H NMR where the OH-6 protons 'observe' the solvent. Such a structuring would involve interaction in the bilayer of the alkyl chains, and should lead to inequivalence for the O-2 and O-3 chains. This structure is in agreement with the observation of a phase change between 40 and 60 °C, for the CH_2 chain resonances, which is proposed to arise from transition between a non-mobile (gel state) and a dynamic (fluid) state.

Particularly strong evidence supporting an inverse membrane structure in THF and a normal membrane structure in pyridine comes from the use of external shift reagents. These cause perturbations in the ^{1}H NMR spectra by a through-space mechanism and thus will affect the regions of the aggregates in contact with the solvent in THF. It is the alkyl chain resonances which are perturbed, hence an inverse structure should exist. In pyridine where the normal bilayer structure will cause the alkyl chains to be buried no effects are observed for these resonances, but here the OH-6 head group resonance is strongly perturbed. In the case of $Eu(NO_3)_3$ THF the small cation is apparently capable at high concentrations of penetrating the aggregate and interacting with OH-6 head group moieties.

Further support for the difference in the nature of the aggregates found in THF and pyridine arises from surface area–pressure isotherms obtained from deposition of THF and pyridine solutions of β-CD-C12 diester at the water surface. For deposition of a THF monolayer a value of $A = 368$ Å^2 is obtained, corresponding closely to that observed for deposition of

chloroform solutions. For deposition of pyridine solutions an apparent $A = 180$ Å^2 is observed. This may arise for partial dissolution of the deposited compound by the miscible pyridine, but THF is also miscible and similar effects might be expected if only a dissolution effect were occurring. Even in chloroform head group–head group interactions undoubtedly occur and the dispersion of this structure to give a monolayer is favoured by the hydrophobic interaction between the alkyl chains and water and hydrogen bonding of the hydroxyl groups with water. Similar effects will occur for THF even with possible dissolution of THF in water.

For pyridine the interactions within the organized systems in which the polar head groups are oriented to the exterior and the lipophilic chains are blocked from solvent interaction will be less favourable to the formation of monolayers and either partial dissolution of the aggregates or deposition of multilayers will be favoured; either event will lead to a reduction in the observed A_0. The exact nature of this process is currently under investigation.

The formation of monolayers by amphiphilic CDs has been observed for compounds having hydrophobic groups substituted at the primary face.[5,16,18,19] For such compound highly unstable layers were observed for chain lengths of less than six carbon atoms; in this study stable layers were observed even for the β-CD-C2 diester.

For chain lengths of 6–12 carbon atoms collapse pressures are approximately equal, with a subsequent increase in stability for the β-CD-C14 ester. Whereas the α-CD-C14 and β-CD-C14 diesters collapse at similar pressures, γ-CD-C14 forms more stable layers.

Collapse of the monomolecular layers should lead to the formation of multi-layered aggregates at the air–water interface. Two factors should govern such a collapse: first, the adhesion forces at the water surface, and second, the depth of the molecule. From the above results it would seem that either factor may predomi-

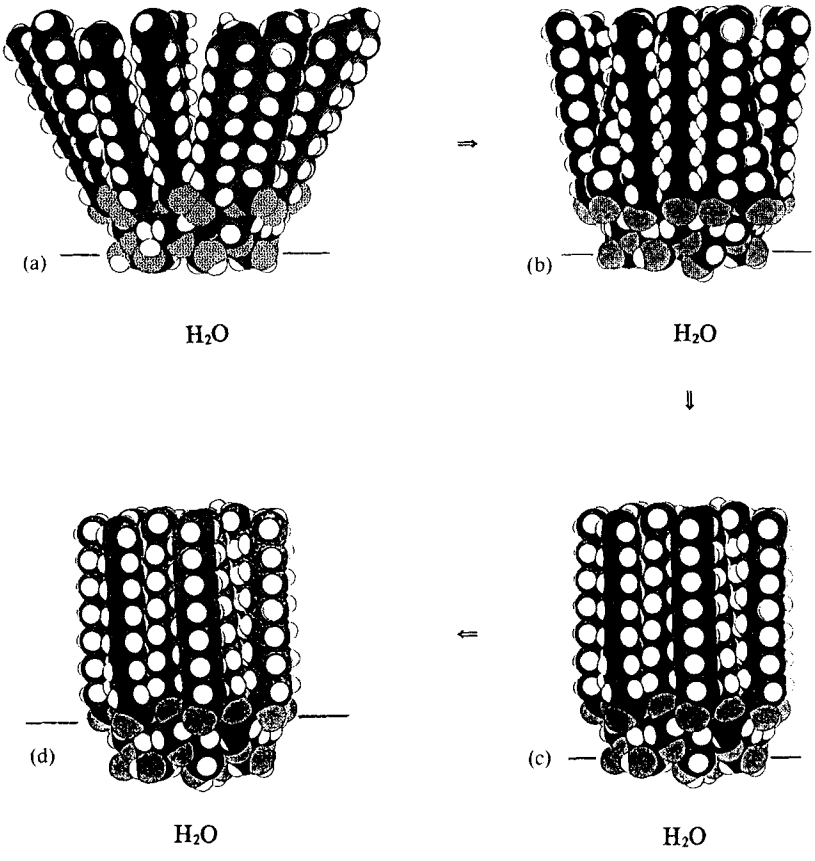

Figure 13. Proposed states at the air–water interface for C14 diesters: (a) expanded; (b) non-compact; (c) compact; (d) compact–immersed

nate; the observation of equivalent collapse pressures for β-CD-C6 through β-CD-C12 suggests that adhesion forces are important in these cases. For the passage from α-CD through β-CD to γ-CD the molecular depth would appear to be important for α-CD and β-CD (increasing surface area, same stability); whereas with γ-CD the adhesion forces are important (larger surface area, greater stability).

Within the zone of increasing pressure, in addition to reorganization of the chain packing it may be expected that the CD amphiphile molecule will reorient themselves with respect to the water surface, changing from a possible tilted orientation to an upright form accompanied by possible immersion of the head group in the solvent phase. In such an orientation, hydrogen bonding would become possible between water molecules and the O-4 and O-5 carbohydrate oxygens; interactions of this type have been observed in the herring-bone β-CD crystal structures.[20,21]

For the C14 diesters in particular, a less compact state is observed at low compression pressures; this may correspond to a liquid expanded state[15] in which the acyl chains will be in fluid (non-oriented) conformations. The stability of such a state will be related to the chain melting temperature and hence chain length; as this is a phase change at a monomolecular surface, this temperature should not be related to the phase change temperature observed in the pyridine 'membrane' structures. Figure 13 show schematically the transition from an open through a non-compact to a compact state.

The molecular graphics studies support the possibility of the chains rearranging geometry to give a compact form in which the acyl groups are close packed. The availability of the carbonyl and cyclodextrin ring oxygen atoms to interact with the solvent leads to speculation about how deeply in the Langmuir layers the polar head group will extend into the water. If significant penetration does happen there will arise a zone several ångstroms deep in which the water is in a bound structure rather than the bulk free state.

CONCLUSION

We have shown that the amphiphilic cyclodextrins having two hydrophobic ester groups at the secondary face are capable of forming organized assemblies in aqueous and non-aqueous solvents and at the air–water interface. At the air–water interface, for the β-CD diesters with relatively short chains the stability is dominated by the presence of the rigid cyclodextrin head group. For compounds with carbon chain lengths of 10 or greater, phase changes involving the alkyl chain are observed and the stabilization of the monomolecular layer by hydrophobic interactions between the chains become important; not only the OH-6 hydroxyl groups would participate in hydrogen bonding to the water but also the ester carbonyl groups would be sterically available for hydrogen bonding. This would effectively place the water surface at the ester group lever; now the OH-6 groups would extend about 8–18 Å into the water and give rise to a zone in which there would be water molecules bound to the cyclodextrin head group and present in a structured rather than bulk free state. The cyclodextrin cavity will probably include one or more solvent molecules in these amphiphilic aggregates. There also evidence for multi-molecular organization within these supra-molecular systems.

ACKNOWLEDGEMENTS

We thank SEDERMA for financial assistance to C.-C.L. an P.Z. This project was supported by the Université de Paris Sud in the context of the Action Interdisciplinaire 'Cyclodextines Amphiphiles'.

REFERENCES

1. J. Szjetli, *Cyclodextrin Technology*. Kluwer Dordrecht (1989).
2. H. Hashimoto, in *Proceedings of the IV International Symposium on Cyclodextrins, Munich*, ed. O. Huber, p. 533–544, Kluwer, Dordrecht (1988).
3. D. Duchene, F. Glomot and C. Vaution, in *Cyclodextrins and Their Industrial Uses*, edited by D. Duchene, Chapt. 6. Editions de Santé, Paris (1987).
4. (a) W. A. Konig, *Kontakte (Darmstadt)* **3** (1991); (b) D. W. Armstrong, M. Hilton and L. Coffin, *LC·GC Int.*, **5**, 28 (1992); (c) V. Schurig and H. P. Nowotny, *Angew. Chem. Int. Ed. Engl.* **29**, 939 (1992).
5. A. W. Coleman, C. C. Ling, P. Zhang, A. Kasselouri, H. Parrot-Lopez, J. Mahuteau, L. Mascrier, A. Baszkin, G. Albrecht, C. de Rango and M. Miocque, in *Proceedings of the Fourth International Symposium on Inclusion Phenomena, Stara Lesna, Czechoslovakia, 1991*, Reseau de Recherche 'Innovation Therapeutique,' Centre Pharmaceutique, Université de Paris Sud, Châtenay-Malabry.
6. P. Zhang, C. C. Ling, A. W. Coleman, H. Parrot-Lopez and H. Galons, *Tetrahedron Lett.* **32**, 2769 (1991).
7. R. B. Gennis, *Biomembranes. Molecular Structure and Function*, Springer, Berlin (1989).
8. C. C. Ling, Doctoral Thesis, Université de Parsi XI (1991).
9. K. Shinoda, T. Yagamuchi and R. Hori, *Bull. Chem. Soc. Jpn.* **34**, 237 (1961).
10. T. Herrington and S. S. Sahi, *Colloids Surf.*, **17**, 103 (1986).
11. A. Meliani, E. Perez, I. Rico and A. Lattes, *New J. Chem.* **15**, 871 (1991).
12. K. Wurthrich, *NMR in Biological Research, Peptides and Proteins*, and references cited therein. North-Holland, Amsterdam (1976).
13. R. C. Warren, *Physics and the Architecture of Cell Membranes*. Hilger, Bristol (1987).
14. K. Harata, *Inclusion Compounds*, Vol. 5, Chapt. 9, and references cited therein. Oxford University Press, Oxford (1991).

15. K. S. Birdi, *Lipid and Biopolymer Monolayres at Liquid Interfaces*. Plenum Press, New York (1989).
16. S. Taneva, K. Ariga, Y. Okahata and W. Tagaki, *Langmuir* **5**, 111 (1989).
17. G. A. Jeffrey and H. Maluszynska, *Carbohydr. Res.* **207**, 211 (1990).
18. Y. Kawabata, M. Matsumoto, M. Tanaka, H. Takahashi, Y. Irinatsu, S. Tamura, W. Tagaki, H. Nakahara and K. Fukuda, *Chem. Lett.* 1933 (1986).
19. M. Tanaka, Y. Ishi zuka, M. Matsumoto, T. Nakamura, A. Yaba, H. Nakanhiaha, Y. Kawabeta, H. Takahashi, S. Tamura, W. Tagaki, H. Nakahara and K. Fukuda, *Chem. Lett.* 1307 (1987).
20. C. H. Betzel, W. Saenger, B. E. Hingerty and G. M. Brown, *J. Am. Chem. Soc.* **106**, 895 (1984).
21. P. Charpin, I. Nicolis, F. Villain, C. De Rango, A. W. Coleman, *Acta Crystallogr., Sect. C* **47**, 1829 (1991).